Multiple Material Microstereolithography

Jae-Won Choi[1,2], Eric MacDonald[2,3], and Ryan Wicker[1,2]

[1]Department of Mechanical Engineering, The University of Texas at El Paso, El Paso, TX 79968

[2]W.M. Keck Center, The University of Texas at El Paso, El Paso, TX 79968

[3]Department of Electrical and Electronic Engineering, The University of Texas at El Paso, El Paso, TX 79968

Abstract

We have previously described the development of a μSL system using a Digital Micromirror Device (DMD™) for dynamic pattern generation and an ultraviolet (UV) lamp filtered at 365 nm for crosslinking the photoreactive polymer solution. The μSL system was designed with x-y resolution of ~2 μm and a vertical (z) resolution of ~1 μm (with practical limitations on vertical resolution of ~30 μm resulting from the current laboratory setup). This μSL system is capable of producing real three-dimensional (3D) microstructures, which can be used in micro-fluidics, tissue engineering, and various functional micro-systems. As has been explored and described in μSL, many benefits will potentially be derived from producing multiple material microstructures in μSL. One particular application area of interest is in producing multiple material micro-scaffolds for tissue engineering. In this work, a method for multiple material μSL fabrication was developed using a syringe pump system to add material to a small, removable vat designed for the μSL system. Multiple material fabrication was accomplished by manually removing the vat and draining the current material, rinsing the vat, placing the vat back into the system, and dispensing a prescribed volume in the vat using the syringe pump. Layer thicknesses less than ~30 μm were achieved using this process. To demonstrate this system, several multiple material microstructures were produced, and we believe multi-material μSL represents a promising technology for producing functional microstructures with composite materials.

Keywords: Microstereolithography (μSL), multi-material fabrication

1. Introduction

Microstereolithography (μSL) has been a promising solution for building a 3D microstructure since the first development in 1993 (Ikuta and Kirowatari). The resolution of the system and fabrication capability of complex microstructures have been continuously improved, and various application areas have been being explored (Zissi *et al.* 1996; Bertsch et al. 1997, 2000, 2001, 2004; Sun and Zhang 2002; Lee and Cho 2003; Kang *et al*. 2004; Sun *et al.* 2005; Choi et al. 2006, 2009a, 2009b; Lee *et al.* 2007; Limaye and Rosen 2007; Han *et al*. 2008; Ha et al. 2008; Park *et al*. 2009). The principle of μSL is similar to that of stereolithography (SL) except for the achievable resolution. These μSL systems crosslink a photocurable liquid material with a thin layer (a few μm to tens of μm), so that 3D microstructures can be produced by stacking the crosslinked thin layers in sequence. Most μSL systems use a single liquid material, however many advantages exist with the use of multiple materials in a system. For example, multiple material 3D microstructures can be used for nerve guidance conduits (NGCs) in tissue engineering, which require varying concentration of nerve growth factor (NGF) along the build direction (Arcaute et al. 2007, 2009). Additionally, combining several materials in a microstructure can provide multiple mechanical, chemical, and/or biological properties, which will result in new applications.

In 2001, Ikuta *et al*. first suggested multiple material μSL; however, the system was limited to simple 2.5D microstructures, where two materials were used - with only one material in any given layer. Furthermore, several possible problems were not addressed such as material mixture between two materials and fabrication capability of real 3D microstructures. In order to produce multiple material 3D microstructures, material mixture has to be resolved. Karina *et al.* (2007, 2009) reported multiple material NGCs with the use of a commercial SL system using poly (ethylene glycol) (PEG), where they controlled a layer thickness by manually dispensing a material using a pipette into a custom-made small vat, and washing the current solution before changing to the second solution. Hence, it is proposed that the use of a small vat and automatic dispensing pump in μSL is a solution for producing multiple material microstructures while removing material mixture.

In this work, a multiple material μSL system was developed using a syringe pump system to dispense material to a small, removable vat designed for an existing μSL system. Multiple material fabrication was accomplished by manually removing the vat from the platform and draining the current material, rinsing the vat, placing the vat back into the platform, and dispensing a prescribed volume of a different material into the vat through the syringe. To demonstrate the validity of this system, several multiple material microstructures were produced, and the following describes the development of multiple material μSL system and fabrication of multiple material 3D microstructures.

2. Syringe pump-based projection microstereolithography

2.1 Projection microstereolithography

μSL can be classified with regards to the method of layer formation as either *scanning* - using a focused laser spot - or *projection* - using a projected pattern (Varadan et al. 2001). In this work, a projection μSL using Digital Micromirror Device (DMD^{TM}), which is used for the generation of the light pattern, was employed to produce multiple material 3D microstructures. The system consists of ten component subsystems: 1. a mercury lamp as a light source with output of 200 W (Omnicure S2000^{TM}, EXFO Co., Canada), 2. an optical fiber and collimating lens (EXFO Co., Canada), 3. a DMD^{TM} having ~780,000 micromirrors with the size of 13.68 μm (DMD^{TM} Starter Kit, Texas Instruments, USA), 4. a tube lens with the focal length of 120 mm and the diameter of 40 mm (Achromat doublet lens, MellesGriot Co. USA), 5. reflecting mirror with the diameter of 50.8 mm (Newport Co., USA), 6. a focusing unit with the resolution of 1 μm (IM-4, Nikon Co., Japan), 7. an objective lenses with the Numerical Aperture (N.A.) of 0.13 and 0.3 (CFI Plan Flour 4× and 10×, Nikon Co., USA), 8. a linear Z-stage with the resolution of 1 μm (ATS100-050, Aerotech, USA), 9. a stainless steel platform, and 10. a stainless steel resin vat - all shown together in Fig. 1.

In general, the major steps in the production of 3D microstructures include creation of machining data, fabrication, and post-processing. The machining data, which is a binary image series in projection μSL, is prepared using 3D modeling, STL file conversion, slicing, and then binary image generation depicting sliced sections. In the fabrication process, the binary images are transferred to the DMD™ board in sequence. For each slice, the lamp exposure set to the prescribed duration and Z-stage moved the thickness of the sliced. The DMD™ generates the dynamic mask, by individually tilting each micromirror by ±12° according to the binary value determined from the original design file. In aggregate, all of the micromirrors of the DMD™ project an image for each slice. The patterned light is delivered by the tube and reflecting mirror and focused by the objective lenses. Finally, a cured layer is immersed by lowering the Z-stage and is covered by new resin for the next layer at the prescribed height. After finishing fabrication, a microstructure is washed out with isopropyl alcohol (IPA) and post-cured for ~30 minutes. The typical exposure energy at the resin surface was measured ~26.35 mJ/cm^2 and ~123.9 mJ/cm^2 using the objective lens with the N.A. of 0.13 and 0.3, respectively. Fig. 2 shows fabricated chess pieces from the current system using two different objective lenses and thus demonstrating that the system is well suited for producing 3D microstructures. Furthermore, we recommend the interested readers to read the references (Choi *et al.* 2006, 2009a, 2009b) for further details of the system.

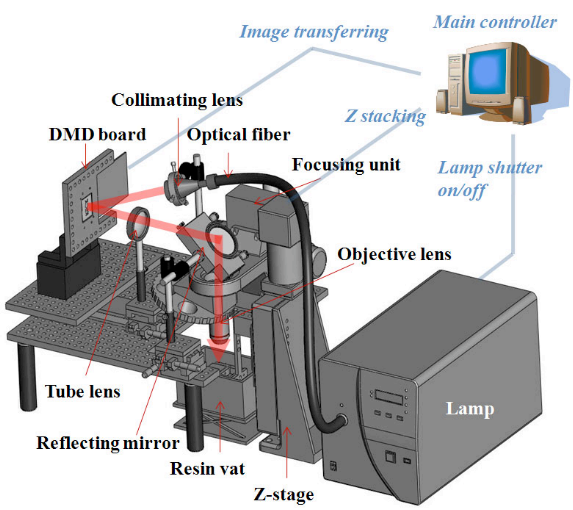

(a)

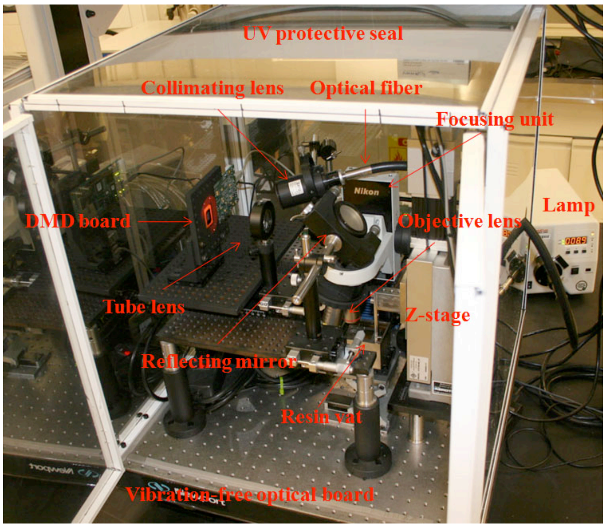

(b)

Fig. 1 Developed μSL system: (a) schematic of the system. (b) photo of the system

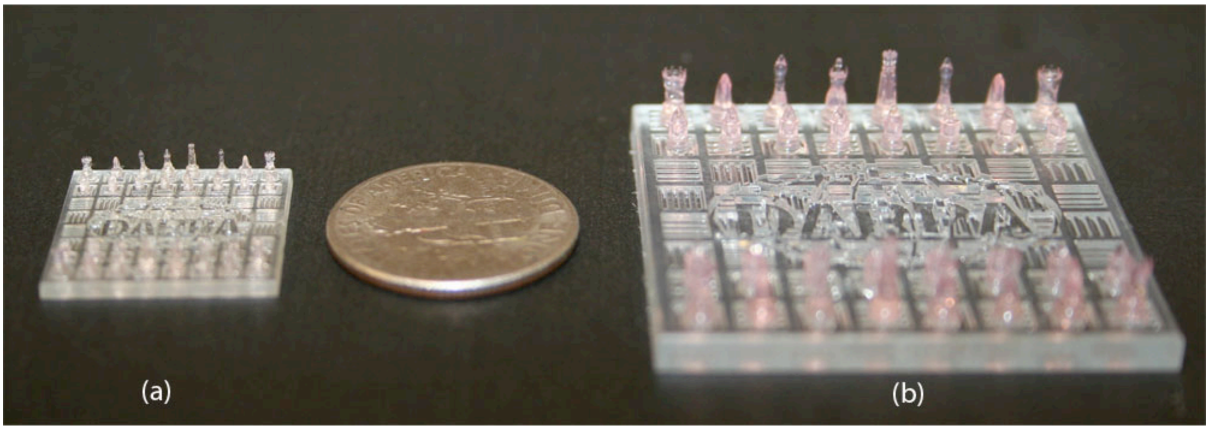

Fig. 2 Fabricated chess piece sets: using the objective lens with the N.A. of (a) 0.3, (b) 0.13. The coin in the middle is dime, and the boards to place pieces were produced out of 3D Systems Viper si2™

2.2 Syringe pump-based projection microstereolithography system

2.2.1 Design of universal platform and cylindrical vat

To utilize a syringe-based pumping subsystem, a small cylindrical vat is required with special platform. In the original μSL system, the platform with the substrate is immersed in a resin, and then moved downward and upward for leveling the resin. In addition, the μSL system was aligned with the prescribed focal length from the objective lens, and thus the position of top surface of the substrate and the bottom surface of the cylindrical vat should be the same to avoid requiring a new alignment. To accomplish this, a universal platform as shown in Fig. 3 was suggested, and it includes two registration planes for the substrate and cylindrical vat. For single material fabrication, a substrate is equipped as shown in Fig. 3 (b) including two spring plungers necessary to secure it. A quartz substrate with the size of 25.4 mm × 25.4 mm × 4 mm was provided from Chemglass Inc. (Vineland, NJ). Alternatively, for multiple material fabrication, a cylindrical vat is placed in the platform as shown in Fig. 3 (c). The index in the cylindrical vat was used for registration after the vat was removed from the platform for rinsing and material changeover and then later placed back in the platform (Karina *et al.,* 2006). The cylinder vat was machined with the inner diameter of 16 mm and the height of 10 mm using stainless steel.

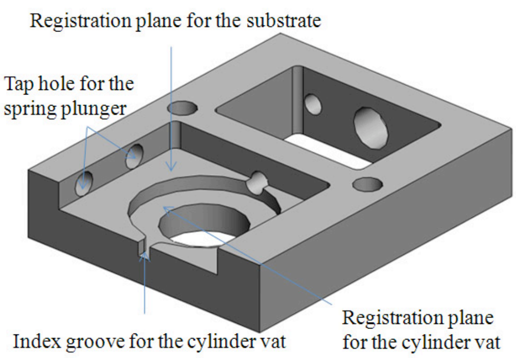

(a)

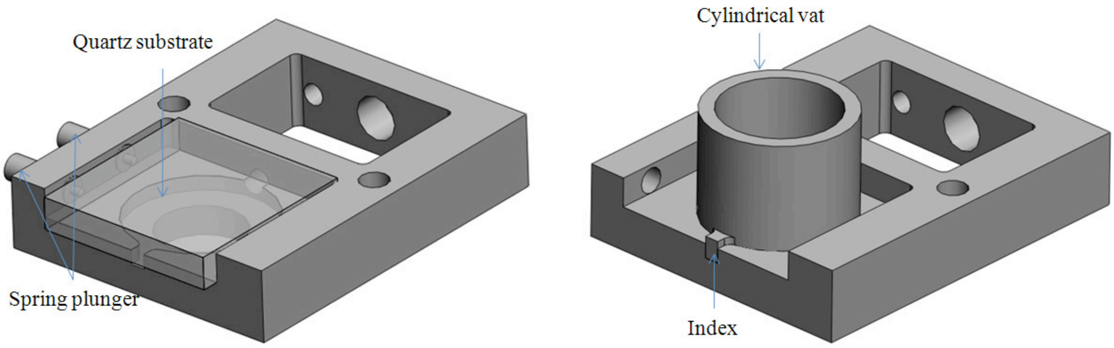

(b) (c)

Fig. 3 Universal platform for a substrate and cylindrical vat: (a) suggested platform, (b) with a substrate, and (c) with a cylindrical vat.

2.2.2 Syringe-based pumping system

A pump (NE-1000) was purchased from New Era Pump Systems Inc., and a 3 ml syringe (BD Inc., Franklin Lakes, NJ) was used. Using these pump and syringe, the dispensing rate can be controlled up to 2.434 μl/hr. To deliver a liquid resin from the syringe to the vat, an infusion set including a 19G needle and 30 cm tube was used. The needle tip was bent to be secured in the vat. To imitate a deep-dip process in μSL, excessive pumping and withdrawing of the solution were conducted with the given volume. If there was no prebuilt microstructure in the vat, the volume for 10 μm layer thickness is ~2 μl. For multiple material fabrication, the volume to be dispensed is determined by calculating the volume of the existing prebuilt microstructure. This can be determined by obtaining the cross-section area of a model.

3. Materials and method

3.1 Materials

For the multiple material fabrication, WaterShed^{TM} 11120, ProtoTherm^{TM} 12120, and 14120 White as commercial resins were provided by DSM Somos$^{®}$ (New Castle, DE, USA), and propoxylated (2) neopentyl glycol diacrylate (PNGD) as the diluent was provided by Sartomer, Inc. (Warrington, PA). For cure depth control, Tinuvin 400 was provided by Ciba Specialty Chemicals (Newport, DE).

3.2 Viscosity control

The WaterShed^{TM} 11120, ProtoTherm^{TM} 12120, 14120 White have the nominal viscosity of ~260 cP, ~410 cP, and ~240 cP at 30 ^{o}C, and it is relatively high for use in μSL given that the recoating cannot be conducted by a sweeper. Thus μSL requires a low viscosity resin for refreshing a resin using a deep-dip process. For reducing the viscosity, diluents was added to the resins, and the viscosity was measured by Brookfield viscometer (DV-E, Middleboro, MA) according to the mixture ratio (100: 0, 90: 10, 80: 20, 70: 30, 60: 40, and 50: 50 (each resin : PNGD)) at room temperature (24 °C). In μSL, a viscosity of 200 cP or less for the photocurable resin was the objective as recommended previously (Varadan *et al.,* 2001; Choi et al., 2009a, 2009b).

3.3 Curing characteristics test

Commercial resins in stereolithography are suitable for producing macrostructures with feature sizes larger than beam diameters of 75 and 250 μm. For cure depth control, Tinuvin 400 as a light absorber was used with the concentration of 0.5 wt% for each resin, and in order to obtain curing characteristics (penetration depth of the light (D_p) and critical energy (E_c)) of the blended resins, curing tests were conducted (Choi *et al.,* 2009a). These curing characteristics were used for setting process parameters such as exposure energy, etc. The curing test was conducted by producing long enough posts and patterning a crossbeam on the posts with varying exposure energy from 210 to 527 mJ/cm^2. Finally D_p and E_c were calculated using the Beer-Lambert formula as defined in Eq. 1, where the depths of the crossbeams according to the exposure energy were measured and used in the equation (Jacobs, 1993).

$$C_d = D_p \ln (E_{max}/E_c) \qquad (1)$$

3.4 Multi-material fabrication

For multiple material fabrication, a chess piece ‘Rook’ as shown in Fig. 4, which consist of three materials, was fabricated. In addition, to verify the capability of multi-material fabrication in a layer, a post and helix were produced.

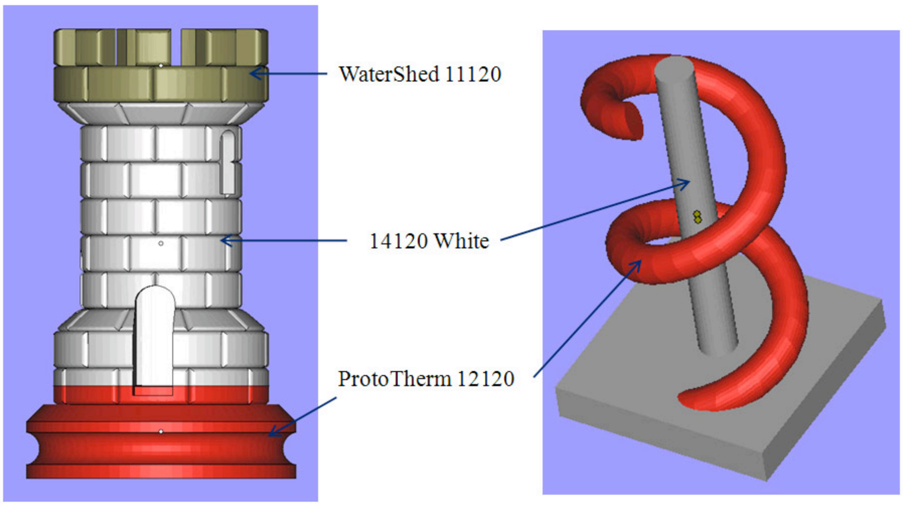

Fig. 4 Multi-material models: (a) chess piece ‘Rook’, and (b) a post and helix

4. Results

4.1 Viscosity

The viscosity of the diluted materials increased as the amount of diluent increased as shown in Fig. 5. The original viscosity of the resins were ~790 cP, ~1100 cP, and 480 cP for WaterShed™ 11120, ProtoTherm™ 12120, and 14120 White, respectively. The mixture ratio of 50:50 of all three materials provided a viscosity of ~100 cP, - obtaining the recommended value for μSL.

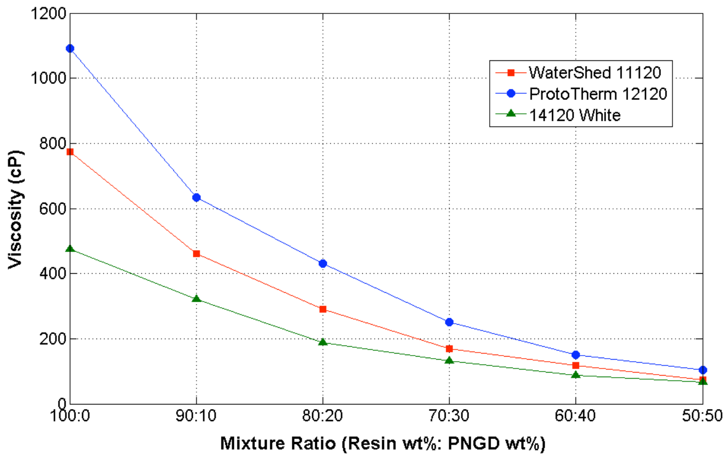

Fig. 5 Viscosity variation according to mixture ratio

4.2 Cure depth control

The semi-log graph as shown in Fig. 6 represents cure depth change according to the variation of exposure energy. The regressed lines were generated to obtain E_c and D_p as curing characteristics, which are shown in Table 1. For the diluted $\text{WaterShed}_{\text{TM}}$ 11120, lower energy levels did not cure crossbeams, and the minimum feature size for all three resins was ~50 μm. To obtain a ~50 μm feature, the exposure time needs to be chosen 12 s (= 318 mJ/cm^2), 8 s (= 212 mJ/cm^2), and 8 s for WaterShed™ 11120, ProtoTherm™ 12120, and 14120 White, respectively.

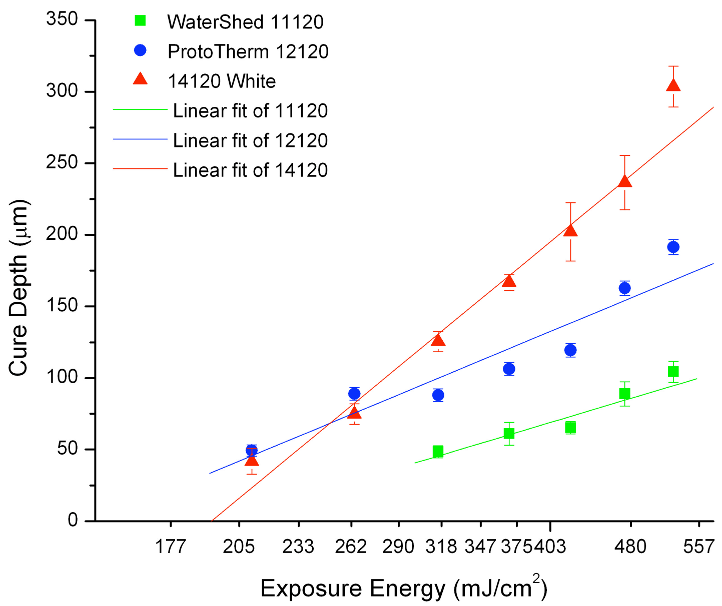

Fig. 6 Cure depth change by varying exposure energy

Table 1 Calculated E_c and D_p for each resin

	D_p (μm)	E_c (mJ/cm^2)
WaterShed™ 11120	96.2	196.9
ProtoTherm™ 12120	133.8	149.9
14120 White	264.9	193.1

4.3 Developed system and single-material fabrication

The step motor-driven pump with a 3 ml syringe was embedded in the current μSL system. Fig. 7 shows the syringe pump subsystem, which dispenses and withdraws the prescribed amount into the vat through the small diameter hose. The bent needle was manually secured around the vat, and the needle tip reaches the bottom of the vat to prevent air bubbles from entering the tip when withdrawn. A chess piece 'King' as shown in Fig. 8 was successfully produced using the developed system.

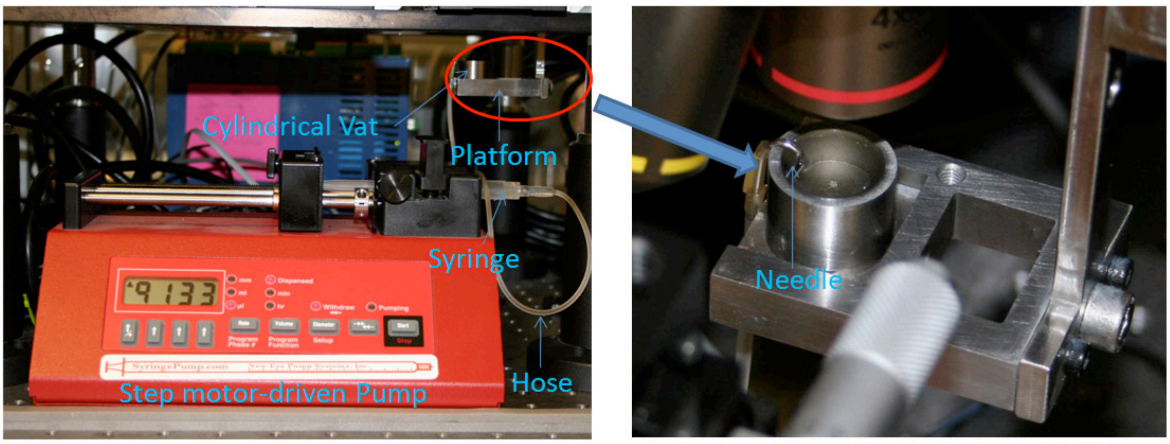

(a) (b)

Fig. 7 Embedded syringe pump subsystem: (a) pump, syringe, hose, and platform; (b) cylindrical vat and bent needle

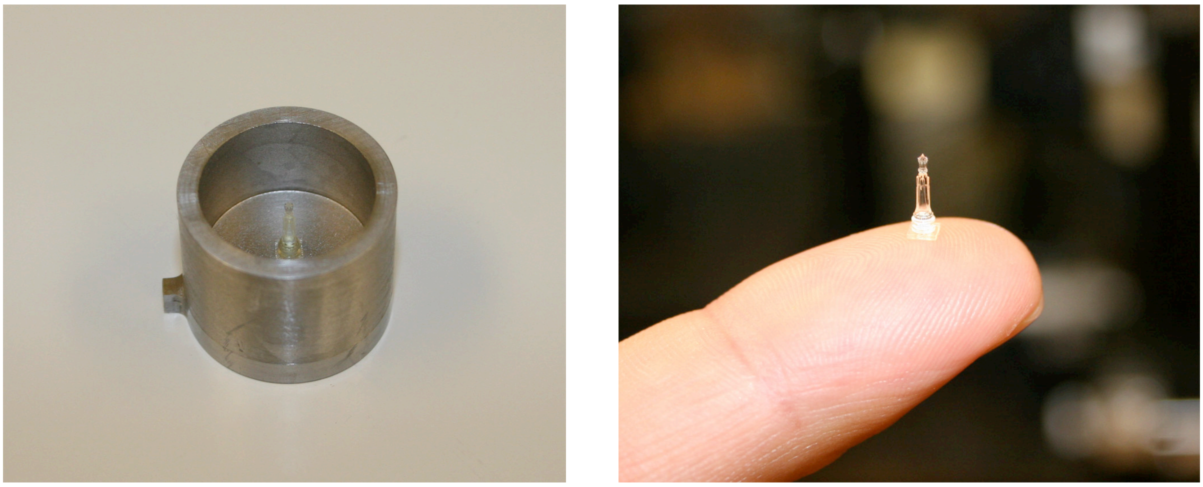

(a) (b)

Fig. 8 Single fabrication: (a) fabricated 'King' piece in the vat, (b) on an index finger.

4.4 Multi-material Fabrication

Using the developed system and diluted materials, a multi-material 'Rook' part as shown in Fig. 9 was produced. Compared to the model as shown in Fig. 4, material was successfully cured on the previously built layer of different material, thus providing compelling evidence that the developed system is capable of producing multi-material microstructures. Additionally, a post and helix parts as shown in Fig. 10 were successfully built, where the post was built first and the helix was built later. These fabrication results show that the developed μSL system with the syringe pump can successfully produce multi-material 3D microstructures.

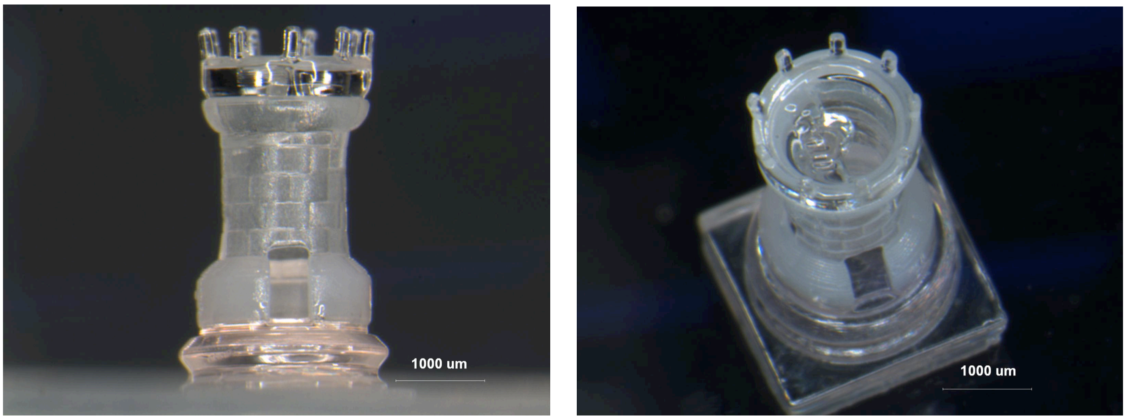

(a) (b)

Fig. 9 Fabricated 'Rook' using multi-material: (a) front, and (b) perspective view

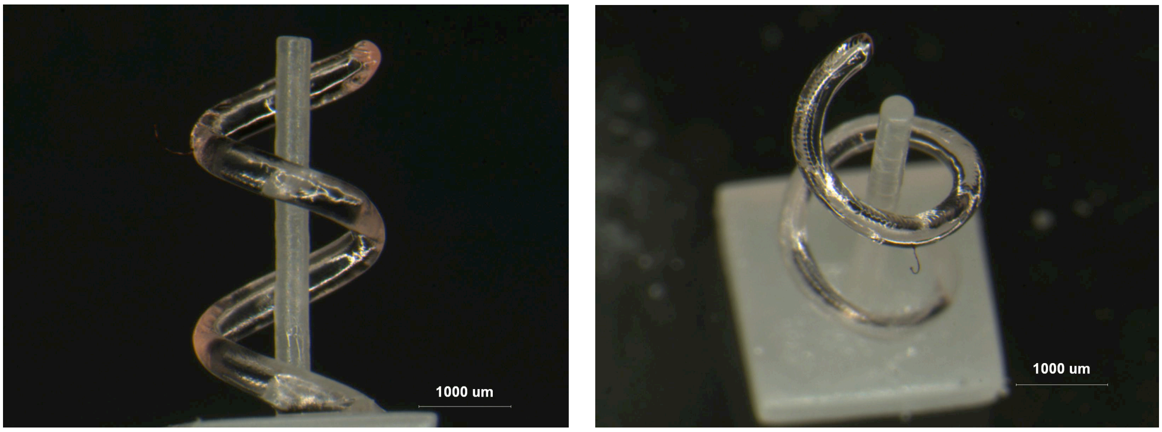

Fig. 10 Fabricated a post and helix: (a) front view, and (b) perspective view

5. Conclusions

In this work, the development of multiple material μSL system was demonstrated which included a syringe pump subsystem. The syringe pump was installed in an existing μSL system, and material was delivered through a hose with a needle, which was secured to a vat. For the pumping subsystem, a universal platform was developed, where a rectangular quartz substrate for single material fabrication or a small cylindrical vat with an index for multiple material fabrication were selectively equipped. Three commercial resins for multiple material were provided and diluted to provide low viscosity. Additionally, a light absorber was added to control cure depth, and curing characteristics were investigated. In order to confirm the ability to dispense, a single material microstructure was produced. Finally using the prepared three materials, a multiple material microstructure was successfully produced by changing materials between builds. In conclusion, the developed multi-material μSL is clearly a promising technology for producing functional microstructures with composite materials.

References

Arcaute K; Mann BK; Wicker RB (2006) Stereolithography of three-dimensional bioactive poly(ethylene glycol) constructs with encapsulated cells. Annals of Biomedical Engineering 24 (9): 1429-1441

Arcaute K; Zuverza N; Mann B; Wicker R (2007) Multi-material stereolithography: spatially-controlled bioactive poly(ethylene glycol) scaffolds for tissue engineering. Proc of 18Th Annual Solid Freeform Fabrication Symposium, Austin, TX: 458-469.

Arcaute K; Mann BK; Wicker RB Stereolithography of spatially-controlled multi-material bioactive poly(ethylene glycol) scaffolds. Acta Biomaterialia, to appear (Manuscript No. AB-09-365)

Bertsch A; Zissi S; Jezequel JY; Corbel S; Andre JC (1997) Microstereophotolithography using a liquid crystal display as dynamic mask-generator. Microsystem Technologies 3 (2): 42-47

Bertsch A; Bernhard P; Vogt P; Renaud P (2000) Rapid prototyping of small size objects. Rapid Prototyping Journal 6 (4): 259-266

Bertsch A; Zissi S; Jezequel JY; Corbel S; Andre JC (2001) Microstereolithography: concepts and applications. Proc of 8th IEEE International conference on Emerging Technologies and Factory Automation: 289-298

Bertsch A; Jiguet S; Renaud P (2004) Microfabrication of ceramic components by microstereolithography. Journal of Micromechanics and Microengineering 14: 197-203

Choi JW; Ha YM; Lee SH; Choi KH (2006) Design of microstereolithography system based on dynamic image projection for fabrication of three-dimensional microstructures. Journal of Mechanical Science and Technology 20 (12): 2094-2104

Choi JW; Wicker RB; Cho SH; Ha CS; Lee SH (2009) Cure depth control for complex 3D microstructure fabrication in dynamic mask projection microstereolithography. Rapid Prototyping J. 15 (1): 59-70

Choi JW; Wicker R; Lee SH; Choi KH; Ha CS; Chung I (2009) Fabrication of 3D biocompatible/biodegradable micro-scaffolds using dynamic mask projection microstereolithography. J. Mater. Process. Technol. 209: 5494-5503

Ha YM; Choi JW; Lee SH (2008) Mass production of 3-D microstructures using projection microstereolithography. J. Mech. Sci. Technol. 22 (3): 514-521

Han LH; Mapili G; Chen S; Roy K (2008) Projection microfabrication of three-dimensional scaffolds for tissue engineering. Journal of Manufacturing Science and Engineering. 130 (2): 021005-1-4

Ikuta K; Kirowatari K (1993) Real three dimensional micro fabrication using stereo lithography and metal molding. Proc of 6th IEEE Workshop on Micro Electro Mechanical Systems (MEMS'93), New York, NY: 42-47

Ikuta K; Maruo S; Ninagawa T (2001) Multi-polymer microstereolithography for hybrid opto-MEMS. Proc of 14th IEEE international conference on micro electro mechanical systems (MEMS 2001): 151-154

Inamdar A; Magana M; Medina F; Grajeda Y; Wicker R (2006) Development of an automated multiple material stereolithography machine. Proc of 17th Annual Solid Freeform Fabrication Symposium, Austin, TX: 624-635

Jacobs PF (1993) Rapid Prototyping and Manufacturing: Fundamentals of Stereolithography, McGraw-Hills, New York, NY.

Kang HY; Lee IH; Cho DW (2004) Development of an assembly-free process based on virtual environment for fabricating 3D microfluidic systems using microstereolithography technology. Journal of Manufacturing Science and Engineering 126: 766-771

Lee IH; Cho DW (2003) Micro-stereolithography photopolymer solidification patterns for various laser beam exposure conditions. International Journal of Advanced Manufacturing Technology 22: 410-416

Lee SJ; Kang HW; Kang TY; Kim B; Lim G; Rhie JW; Cho DW (2007) Development of a scaffold fabrication system using an axiomatic approach. J. Micromech. Microeng. 17: 147-153

Limaye AS; Rosen DW (2007) Process planning method for mask projection micro-stereolithography. Rapid Prototyping Journal 13 (2): 76-84

Park IB; Choi JW; Ha YM; Lee SK (2009) Multiple fabrications of sacrificial layers to enhance the dimensional accuracy of microstructures in maskless projection microstereolithography. International Journal of Precision Engineering and Manufacturing 10 (1): 91-98

Sun C; Zhang X (2002) Experimental and numerical investigations on microstereolithography of ceramics. Journal of Applied Physics 92 (8): 4796-4802

Sun C; Fang N; Wu DM; Zhang X (2005) Projection micro-stereolithography using digital micro-mirror dynamic mask. Sensors and Actuators A: Physical 121 (1): 113-120

Varadan VK; Jiang X; Varadan VV (2001) Microstereolithography and Other Fabrication Techniques for 3D MEMS, John Wiley & Sons, West Sussex, England

Wicker RB; Medina F; Elkins CJ (2004) Multiple material micro-fabrication: extending stereolithography to tissue engineering and other novel application. Proc of 15th Annual Solid Freeform fabrication Symposium, Austin, TX: 754-764.

Zissi S; Bertsch A; Jezequel JY; Corbel S; Lougnot DJ; Andre JC (1996) Stereolithography and microtechniques. Microsystem Technologies 2 (2): 97-102